Available online at www.sciencedirect.com
SCIENCE DIRECT®
C. R. Mecanique 333 (2005) 739–745
COMPTES RENDUS MECANIQUE
http://france.elsevier.com/direct/CRAS2B/

Identification of the convective instability in a multi-component solution by 3D simulations

Viatcheslav V. Kolmychkov [a], Olga S. Mazhorova [a], Yurii P. Popov [a], Patrick Bontoux [b], Mohammed El Ganaoui [c,*]

[a] *Keldysh Institute of Applied Mathematics RAS, 4, Miusskaya pl., Moscow 125047, Russia*
[b] *UMR CNRS 6181, les universités d'Aix–Marseille, 38, rue F. Joliot Curie, 13451 Marseille, France*
[c] *SPCTS UMR CNRS 6638, université de Limoges, 123, avenue Albert-Thomas, 87060 Limoges, France*

Received 24 August 2005; accepted 30 August 2005

Presented by René Moreau

Abstract

Three-dimensional calculations have been done to simulate the onset of convective motion in ternary nondilute solution under phase transition conditions. The process is considered for Rayleigh number in the range $[1 \times 10^3, 1.4 \times 10^4]$, where subcritical convective motion with hexagonal flow pattern is identified. The results are in good agreement with the linear and finite amplitude theory of hydrodynamics instability. ***To cite this article: V.V. Kolmychkov et al., C. R. Mecanique 333 (2005).***
© 2005 Académie des sciences. Published by Elsevier SAS. All rights reserved.

Résumé

Identification d'instabilités convectives dans une solution muticomposants à partir de simulations 3D. Le présent papier concerne les résultats numériques des instabilités de convection naturelle dans un système ternaire en changement de phase. Les simulations sont effectuées en configuration tridimensionnelle. Une bifurcation sous critique avec des cellules hexagonales est identifiée dans la gamme des nombres de Rayleigh $[1 \times 10^3, 1{,}4 \times 10^4]$. Les résultats de simulation sont en bon accord avec les prédictions de la théorie de stabilité linéaire et d'amplitude finie. ***Pour citer cet article : V.V. Kolmychkov et al., C. R. Mecanique 333 (2005).***
© 2005 Académie des sciences. Published by Elsevier SAS. All rights reserved.

Keywords: Computational fluid mechanics; Instability and transitions

Mots-clés : Mécanique des fluides numérique ; Instabilité et transition

Version française abrégée

Dans ce travail, un processus de transition de phase dans un système multicomposants est considéré par étude numérique. Le processus instationnaire est simulé numériquement et les résultats sont comparés aux prédictions théo-

* Corresponding author.
E-mail addresses: magor@keldysh.ru (O.S. Mazhorova), ganaoui@unilim.fr (M. El Ganaoui).

1631-0721/$ – see front matter © 2005 Académie des sciences. Published by Elsevier SAS. All rights reserved.
doi:10.1016/j.crme.2005.08.004

riques liés à l'étude des instabilités dans une couche de fluide horizontale infinie en présence d'un profile non linéaire d'une quantité scalaire au repos (concentration d'espèces dans notre cas) [4,5].

La convection est étudiée dans un domaine parallèllepipédique $L_x = L_y = 25$ mm, la hauteur H peut étre variée en maintenant un grand rapport de forme du domaine d'étude L_x/H au voisinage de 23 pour permettre des confrontations aux résultats théoriques de R. Krishnamurti [4,5]. Au fond du domaine le substrat $A_x B_{1-x} C$ est placé. A la température initiale T_0, la solution est saturée et en équilibre avec le substrat. A l'interface solide/liquide, les compositions satisfont le diagramme de phase. Des conditions de non glissement sont imposées à l'ensemble de la frontière du domaine.

Deux temps caractéristiques sont considérés : le temps dynamique $t_\nu = H_0^2/\nu$ (ν viscosité cinématique du fluide) et le temps diffusif $t_D = H_0^2/D$ (D coefficient de diffusion, identique pour les deux composants) respectivement pour $H_0 = 1$ mm. Le paramètre $\eta = \alpha\lambda(T)$, α est désigne le taux de refroidissement, $\lambda(T)$ étant la pente du diagramme de phase [4]. Le nombre de Rayleigh est considéré dependant du temps $Ra(t) = g\beta H^3 \delta C(t)/(D\nu)$ où $\delta C(t)$ est la différence de concentrations moyennes estimée à partir des calculs. β étant le coefficient d'expansion solutale. Les valeurs du nombre de Rayleigh correspondant aux composants A et B diffèrent de plus d'un ordre de grandeur, le plus grand est considéré (celui de A). Le nombre de Schmidt $Sc = \nu/D$ est égal à 50. Initialement le fluide de composition uniforme dans l'espace et en équilibre avec le substrat.

Le système conservatif des équations de Navier–Stokes et des espèces (la solution de l'équation de l'énergie se ramenant ici à un profil analytique trivial) est résolu dans le cadre d'une approche de type volumes finis de second ordre en espace et en temps. Une méthode de projection est utilisée pour le couplage vitesse pression [7]. Une grille de $100 \times 100 \times 30$ et un pas de temps de $0{,}5 \times t_\nu$ répondent aux exigences de solution numérique indépendantes de la discrétisation spatio-temporelle suite à une série de validations (notamment au voisinage des seuils critiques) [10,11].

Il est intéressant d'établir sous les mêmes conditions les seuils de transitions en configuration bidimensionnelle. Un $Ra_c^{2D} = 1545$ est évalué, en bon accord avec les estimations théoriques $Ra_c = 1537{,}5$ [1]. En 3D, le cas stationnaire est identifié pour $H < 1$ mm. Le seuil de convection est observé pour $H = 1{,}1$ mm après $t_0 = 2{,}1t_D$. La transition illustrée sur la Fig. 2 où l'évolution de l'énergie cinétique est représentée. La convection croit lentement pour $2{,}1t_D < t < 3t_D$, une croissance rapide est notée entre $3t_D$ et $4{,}2t_D$. Quand l'énergie cinétique atteint son maximum, un système de rouleaux primaires auxquels se superpose perpendiculairement une rangée de rouleaux secondaires compose l'écoulement. L'intersection des rouleaux produit des cellules carrées avec un fluide arrivant au centre et descendant sur la periphérie (Fig. 4). Au delà de la valeur maximale de l'énergie cinétique, la transition de la convection bimodale à celle multicellulaire commence pour atteindre un régime développée vers $t = 12{,}3t_D$ (Figs. 3 et 4) suivi d'une transition vers une configuration en cellules hexagonales dont la répartition atteint un régime uniforme vers $t = 37t_D$ (Fig. 4). Les distortions sont uniquement obsérvée sous l'effet de bord. Dans les zones sombres la concentration des especes dissoutes est faible et le transport s'effectue vers le haut pour la solution légère. L'écoulement est stable et observé au delà de $t = 96t_D$. En accord avec la théorie linéaire, après son initiation, la convection tend vers des cellules bidimensionnelles en transition sous l'effet de l'amplification de l'instabilité vers des structures hexagonales (les seules stables au voisinage du Ra critique). L'orientation de l'écoulement est en bon accord avec les prédictions théoriques.

L'évolution de Ra/Ra_c est tracée sur la Fig. 5. Le nombre de Rayleigh augmente pour atteindre la valeur de 1263 puis décroit vers une valeur asymptotique de 1100. C'est 40% plus faible que la valeur critique donnée par la théorie linéaire et 30% plus faible que les prédictions 2D.

Les présents résultats s'interprétent comme l'identification grâce à l'approche 3D, d'une instabilité se produisant à une valeur critique inférieure à celle prédite par la théorie linéaire. L'apparition de convection de configuration hexagonale est un processus complexe nécessaire à la transition.

1. Problem description

Numerical study of mass-transfer in multicomponent systems with phase transition is one of the most challenging problems for Computational Fluid Dynamics. The investigations in this field are encouraged for instance by the requirements of the modern crystal growth technology. Experimental data, as well as theoretical analysis, prove the important role that natural convection plays in different crystal growth techniques forming the mass transport toward the solidification front. Convection usually is an undesirable factor adversely affecting the growth conditions. In most cases diffusive regimes are preferable for the grown material properties. Therefore evaluation of the stability

threshold for the transition from the diffusive mode to the convective one is of primary importance for the designing well controlled crystal growth techniques. Also it contributes to the stability theory of convective motion.

The problem under consideration is the onset of convection in the ternary nondilute alloy under phase transition. It is supposed that solidification occurs in quasi-equilibrium regime (i.e. compositions of the two phases at the solid/liquid interface are related by phase diagram of the system).

A solution of the components A and B in the molten C is enclosed in the parallelepiped box. Horizontal side lengths are $L_x = L_y = 25$ mm, the vertical size H is changed in a range maintaining the aspect ratio of the domain $L_x/H \approx 23$. At the bottom, the substrate $A_X B_{1-X} C$ is placed. At the initial temperature T_0 the solution is saturated and in equilibrium with the substrate. The growth is realized through the gradual system cooling. Under the temperature changes, initially saturated solution becomes supersaturated. Local equilibrium at the solid/liquid interface restores forming the new solid layer at the substrate. Interface concentrations of the two phases assume values compatible with the phase diagram and mass conservation, while the bulk of the liquid retains supersaturated. Qualitative behaviour of concentration distribution is shown in Fig. 1. Growth onto a horizontal substrate necessary involves the generation of nonlinear concentration profile and leads to density gradient normal to the substrate. It can be stable, if the solvent has a greater density than the solutes, and unstable, if the densities are differently disposed. Here we consider the last case and suppose both components A and B contribute to instability. Being sufficiently large unstable density gradient may produce convection [1,2].

The process is described by 3D time-dependent incompressible Navier–Stokes equations in Boussinesq approximation and mass transport equations written for two dissolved components.

In Cartesian coordinates (x, y, z), the dimensionless governing equations take the form:

$$\begin{aligned} &\partial_t V + (V \cdot \nabla)V = -\nabla p + \Delta V + \sum_{i=1}^{2} Gr_i C_i e_z \\ &\nabla \cdot V = 0 \\ &\partial_t C_i + (V \cdot \nabla)C_i = \frac{1}{Sc_i} \Delta C_i \end{aligned} \tag{1}$$

where $\partial_\xi \equiv \frac{\partial}{\partial \xi}$, $\nabla = (\partial_x, \partial_y, \partial_z)$, $\Delta = \nabla^2 = \partial^2_{xx} + \partial^2_{yy} + \partial^2_{zz}$, $(x, y, z) \in \mathcal{D}$, $\mathcal{D} = [0, L_x] \times [0, L_y] \times [0, H]$, $V = (V_x, V_y, V_z)$ is the velocity vector, p is the pressure, C_i, $i = A, B$, is the concentration of the correspondent component dissolved in the liquid phase, $e_z = (0, 0, -1)$, Gr_i is the solutal Grashoff number, Sc_i is the Schmidt number. $Gr_A/Gr_B \approx 10$, $Sc_A = Sc_B = 50$.

The non-dimensional variables are introduced by scaling respectively, the length with the depth of the liquid phase H, the time with H^2/ν, and the concentration with the initial value of the components in the solution.

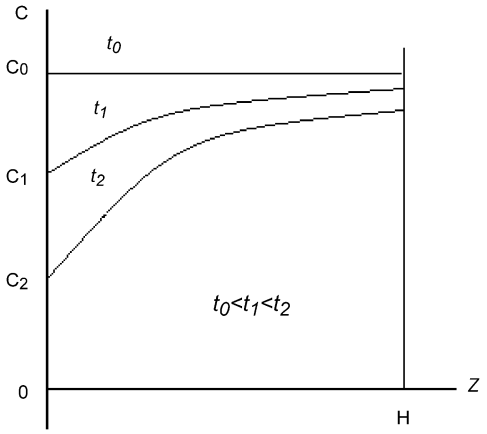

Fig. 1. Illustration of concentration profile evolution inside the liquid layer. C_0, C_1, C_2 equilibrium concentration at the interface for successive time moments.

Fig. 1. Illustration de l'évolution du profile de concentration dans une couche liquide. C_0, C_1, C_2 concentrations d'équilibre à l'interface pour trois instants successifs.

The boundary condition for concentrations are $\partial_n C_i = 0$ everywhere except for $z = 0$, n is a vector normal to a boundary. The phase transition takes place on the substrate ($z = 0$). Change of the liquid volume caused by the film growth is neglected. The conditions at the solid/liquid interface represent the mass balance between the transported and incorporated solute species:

$$\partial_n C_i = V_{\mathrm{gr}} Sc_i (C_i^s - C_i), \quad i = A, B \tag{2}$$

and phase diagram representing the equilibrium between the solution and growing layer:

$$F_{\mathrm{liq}}(C_i, T) = 0, \qquad F_{\mathrm{sol}}(C_i^s, C_i, T) = 0 \tag{3}$$

where V_{gr} is interface rate, C_i^s is concentration of the correspondent solute specie incorporated into the solid phase, and T the temperature of the system. The detailed description of the phase diagram is given in [2].

The temperature gradually decreases with time, while its distribution remains uniform throughout the space. This assumption is approved by high thermal conductivity of the liquid phase and slow cooling. Temperature changes displace the phase equilibrium at the interface producing a solutal gradient in the vicinity of the growing layer and sustaining solidification. The temperature changes as following: $T(t) = T_0 - \alpha t$, where α is the cooling rate and t the time. The boundary condition on velocity field is $V = 0$.

2. On the finite amplitude instability

The onset of convection in the described system has a known so far analogy. Neglecting the existence of the component with smaller Grashoff number, let it be component B, and supposing linearity of phase diagram, we actually obtain the problem concerning convective instability in a horizontal fluid layer with nonlinear undisturbed profile of active scalar quantity (concentration).

A deep insight into the problem is given in [3–5]. Krishnamurti has investigated the onset of convection in the infinite horizontal layer with temperature, as an active quantity, steadily changing on the boundaries at a rate η. It represents the case in which the static state temperature profile is parabolic and its shape is independent on time. The mean temperature of the fluid is changing at the same rate as the boundaries.

The main results of finite amplitude stability analysis relative to the case has been obtained in [4] and can be summarized as:

- In the limit to infinitesimal amplitude, the critical Rayleigh number corresponding to a nonlinear undisturbed profile takes the form $R_{\mathrm{cr}} = R^{(0,0)} + \eta^2 R^{(0,2)}$, $R^{(0,2)} < 0$. For two rigid boundaries $R^{(0,0)} \approx 1708$, that is the well known value for the stability threshold for constant mean temperature [6], $R_{\mathrm{cr}} = 1537.5$ for the dimensionless value $|\eta| = 8$.
- For two-dimensional rolls, as well as for the other flow patterns, except hexagonal cells, linear stability theory would correctly predict the lowest Rayleigh number R_{cr}, at which the fluid is unstable. Near the critical point stationary rolls solution is unstable, when $\eta \neq 0$.
- For hexagonal plan form, motion is possible below R_{cr}, i.e. subcritical convection can be registered. The static state is unstable to finite amplitude disturbances, since infinitesimal perturbation are known to decay below R_{cr}. There is a range of Rayleigh number for which steady state hexagonal flows are stable with the direction of the flow determined by the sign of η. If $\eta < 0$ the direction of the flow in the center of hexagonal cell is upward (the cells of l-type), and downward if $\eta > 0$ (the cells of g-type).

The results of classical stability theory are used to evaluate the simulation data on the development of convection in ternary alloy under phase transition conditions. Here, concentration plays the role of active scalar quantity usually referred to temperature [3,4]. Concentration evolution at the interface is governed by the parameter $|\tilde{\eta}| = |\lambda(T)\alpha|$, where $\lambda(T)$ is the slope of phase diagram, α is a cooling rate; $\tilde{\eta}$ can be treated as the temperature changing rate η in [4]. Though, it should be emphasized that classical stability theory deals with constant η and stationary solutions, while in our case $\tilde{\eta}$ varies with time and the process is time dependent.

3. Numerical results

The development of convective motion is computed. The numerical procedure has been described elsewhere [7].

To analyze the results we introduce the diffusion time scale $t_D = H_0^2/D_A$, $H_0 = 1$ mm, and the actual Rayleigh number that is time dependent and based on the averaged concentration difference observed in the calculations: $Ra(t) = g\beta_A H_0^3 \delta C_A(t)/(D_A \nu)$. $\delta C_A = C_{A,\mathrm{av}}|_{z=H} - C_{A,\mathrm{av}}|_{z=0}$, where $C_{A,\mathrm{av}}$ is average over the correspondent plane concentration of the component A, β_A is the solutal expansion coefficient, ν is the solution viscosity, D_A is diffusion coefficient. In all runs we keep the cooling rate constant and change the liquid depth.

Initially the fluid is at rest, its composition is uniform through out the space and in equilibrium with the substrate. The transition to unsteadiness is allowed to develop from the actual noise that is presented in calculations.

To begin with it is worth establishing a critical depth for the onset of convection in 2D case. Calculations under the same operating conditions (substrate length, cooling rate, phase diagram) allow firstly to register convection at $H = 1.2$ mm in the form of steady rolls [1]. The correspondent value of the Rayleigh number is $Ra_{\mathrm{cr}}^{\mathrm{2D}} = 1545$, for averaged over the processing time $\tilde{\eta} \approx -5$, which practically coincides with $Ra_{\mathrm{cr}} = 1537.5$ for $\eta = -8$ computed in [4]. In 2D configuration, where only rolls are admissible and essentially 3D subcritical convection is impossible, the lowest Rayleigh number beyond which the fluid becomes unstable is predicted by linear stability theory.

In 3D case, calculations show the static state for $H \leqslant 1$ mm. We observed the onset of convection at $H = 1.1$ mm. The temporal evolution of the kinetic energy is plotted in Fig. 2. An unstructured pattern of weak flow has been firstly registered about $t = 2.1t_D$. The convection grows slowly for $2.1t_D < t < 3t_D$. Quick increase in the kinetic energy occurs between $3t_D$ and $4.2t_D$. At the end of this stage, when the kinetic energy reaches its maximum value, the flow deposits in a definite pattern, which consists of a set of primary rolls with a weaker perpendicular set of secondary ones: a bimodal pattern [8,9]. The intersection of the rolls produces square cells. After the kinetic energy passes its maximum a transition from bimodal convection to rolls begins.

The fully-developed flow in the form of rolls establishes about $t = 12.3t_D$. Fig. 3 shows most of the layer with two-dimensional rolls at this time. Remained cells are confined to the two edges of the domain. Then transition from rolls to hexagonal cells begins. The evolution of the planform is very slow. The final pattern of uniform hexagons is established approximately at $t = 37t_D$ (Fig. 4). Distortions of the structure are only observed at the edges. Concentration of the dissolved component is less and the fluid is lighter in dark spots inside hexagons. Bright sides of the cells corresponds to heavier liquid where concentration is larger. The fluid is rising at the center of the cell and falling at the peripheries (the cells of l-type). The flow pattern is stable and observed up to $t = 96t_D$.

Therefore, after initiation the convective motion shows the tendency to two-dimensional rolls. The growing amplitude of the motion and increasing curvature of concentration profile (Fig. 1) make rolls unstable and they break down into hexagons, that are the only stable flow structures near the critical Rayleigh number. The direction of the circulation in the convective cell coincides with R. Krishnamurti's theoretical and experimental results [4,5].

The evolution of $Ra(t)/Ra_{\mathrm{cr}}$ is given on Fig. 5. The calculated Ra reaches the value of 1263, then after the short stability period, drops down and tends to the asymptotic value of 1100. It is about 35% less than linear analysis in the limits of infinitesimal amplitude [4] and 2D calculation predict [1]. These data are in reasonable agreement with the

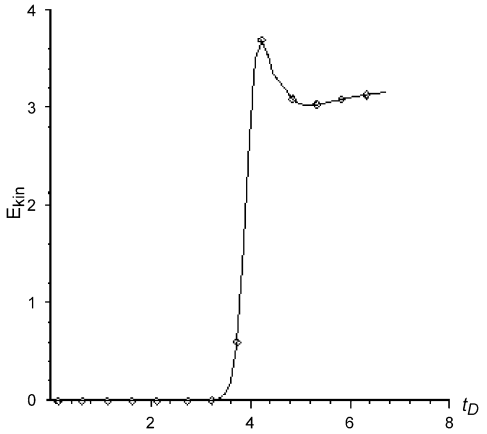

Fig. 2. Temporal evolution of the kinetic energy.

Fig. 2. Evolution de l'énergie cinétique.

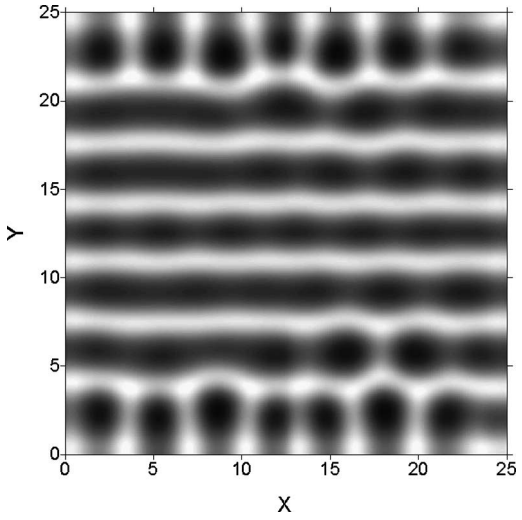

Fig. 3. Concentration distribution in plane $z = H$. Bright spots have higher concentration value then dark ones for $t = 12.3t_D$.

Fig. 3. Distribution de la concentration dans le plan $z = H$. Les spot brillants indiquent une concentration élevée, $t = 12,3t_D$.

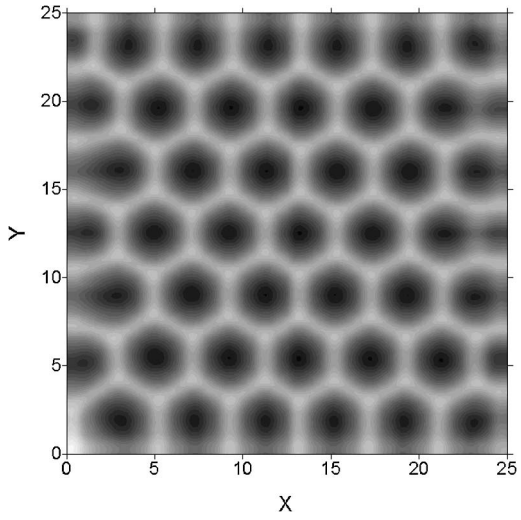

Fig. 4. Concentration distribution in plane $z = H$. Bright spots have higher concentration value then dark ones for $t = 37t_D$.

Fig. 4. Distribution de la concentration dans le plan $z = H$. Les spot brillants indiquent une concentration élevée, $t = 37t_D$.

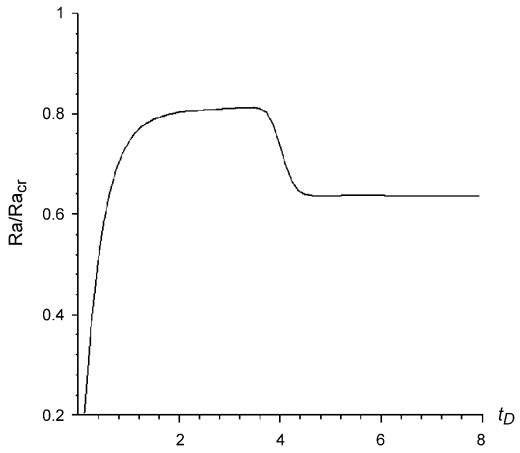

Fig. 5. Temporal evolution of Ra/Ra_{cr}.

Fig. 5. Evolution de Ra/Ra_{cr}.

experimental results [5], where for η from 5 to 10, finite amplitude instability has been observed at Rayleigh number that is near 30% less than critical Ra_{cr}.

The described evolution of fluid motion can be interpreted as a development of finite amplitude subcritical convection occurring at Rayleigh number below the linear stability threshold. Initiation of convection in the form of rolls with ongoing transition to hexagons attributes both to hysteresis gap [3,4] and to evolution of concentration profile: Rayleigh number approaches the critical point decreasing (Fig. 5), while the curvature of concentration profile increases with time (Fig. 1). Both factors contribute to rolls instability and makes hexagonal planform preferable [3–5].

Presented numerical results has been evaluated by a series of calculations on the refined grids. Computations have shown the different time thresholds for convection when the grid size is varied. It should be expected, while convection develops under the noise presented in calculations. Different meshes produce different disturbances which appear to initiate finite-amplitude convection. The situation is absolutely similar to the real experiments on instability [5,8] and

has been registered in numerical simulation also [9]. At the same time flow patterns at the developed stage and integral properties of the solution, such as kinetic energy of the motion, Rayleigh number behaviour, are not affected by grid refinement [10,11]. A $100 \times 100 \times 30$ space grid size and time step $\tau = 0.5t_\nu$ give a good compromise between the CPU and accuracy.

4. Conclusions

Finite amplitude subcritical convection has been registered in 3D computer simulation for solidification of ternary compounds. The calculations are evaluated by the theoretical results on the stability of horizontal layer of fluid with nonlinear undisturbed profile of active scalar function.

The convection starts in the form of rolls at Rayleigh number near the critical one. In our simulation, rolls flow pattern, in agreement with finite amplitude stability analysis, appears to be unstable and breaks down into stable hexagonal flow. The hexagons are established at Rayleigh number less than one predicted by linear theory. The direction of flow circulation in the cell as well as the lowest Rayleigh number at which the static state becomes unstable also correspond with finite amplitude analysis.

References

[1] I.A. Denisov, V.M. Lakeenkov, O.S. Mazhorova, Yu.P. Popov, Numerical study for liquid phase epitaxy of $Cd_xHg_{1-x}Te$ solid solution, J. Crystal Growth 245 (2002) 21–30.
[2] I.A. Denisov, O.S. Mazhorova, Yu.P. Popov, N.A. Smirnova, Numerical modelling for convection in growth/dissolution of solid solution $Cd_XHg_{1-X}Te$ by liquid phase epitaxy, J. Crystal Growth 269 (2004) 284–291.
[3] F.H. Busse, The stability of finite amplitude cellular connection and its relation to an extremum principle, J. Fluid Mech. 30 (4) (1967) 625–649.
[4] R. Krishnamurti, Finite amplitude convection with changing mean temperature. Part I. Theory, J. Fluid Mech. 33 (3) (1968) 445–455.
[5] R. Krishnamurti, Finite amplitude convection with changing mean temperature. Part II. An experimental test of the theory, J. Fluid Mech. 33 (3) (1968) 457–463.
[6] A.V. Getling, Rayleigh–Bernard Correction Structures and Dynamics, World Scientific, Singapore, 1998.
[7] V.V. Kolmychkov, O.S. Mazhorova, Yu.P. Popov, On the solution of Navier–Stokes equations in primitive variables, Preprint No. 60, Keldysh Institute of Applied Mathematics, Moscow, 2001, 39 p.
[8] D.B. White, The planforms and onset of convection with a temperature-dependent viscosity, J. Fluid Mech. 191 (3) (1988) 247–286.
[9] M. Medale, P. Cerisier, Numerical simulation of Benard–Marangoni convection in small aspect ratio containers, Numer. Heat Transfer A 42 (2002) 5572.
[10] V.V. Kolmychkov, O.S. Mazhorova, Yu.P. Popov, Mathematical modelling for convective mass transfer in 3D case, part 1, Preprint No. 92, Keldysh Institute of Applied Mathematics, Moscow, 2003, 28 p.
[11] V.V. Kolmychkov, O.S. Mazhorova, Yu.P. Popov, Mathematical modelling for convective mass transfer in 3D case, part 2, Preprint No. 98, Keldysh Institute of Applied Mathematics, Moscow, 2003, 34 p.